Deriving Mesoscale Temperature and Moisture Fields from Satellite Radiance Measurements over the United States

DONALD W. HILLGER AND THOMAS H. VONDER HAAR

Department of Atmospheric Science, Colorado State University, Fort Collins 80523

(Manuscript received 31 January 1977, in revised form 14 May 1977)

ABSTRACT

The ability to provide mesoscale temperature and moisture fields from operational satellite infrared sounding radiances over the United States is explored. High-resolution sounding information for mesoscale analysis and forecasting is shown to be obtainable in mostly clear areas. An iterative retrieval algorithm applied to NOAA-VTPR radiances uses a mean radiosonde sounding as a best initial guess profile. Temperature soundings are then retrieved at a horizontal resolution of ~70 km, as is an indication of the precipitable water content of the vertical sounding columns. Derived temperature values may be biased in general by the initial guess sounding, or in certain areas by the cloud correction technique, but the resulting relative temperature changes across the field when not contaminated by clouds will be useful for mesoscale forecasting and models. The derived moisture, however, since affected only by high clouds, proves to be reliable to within 0.5 cm of precipitable water and contains valuable horizontal information. Present day applications from polar orbiting satellites as well as possibilities from upcoming temperature and moisture sounders on geostationary satellites are noted.

1. Introduction

High-horizontal-resolution temperature and moisture sounding information has become increasingly necessary for mesoscale research and applications. Both mesoscale forecasting and computer models require a large mass of input data on temperature and moisture. Only recently has this data become available from high resolution sounders such as the Vertical Temperature Profile Radiometer (VTPR) on NOAA operational satellites. However, the calibrated radiances are not used operationally to produce temperature profiles over the land masses, but only over data-sparse regions of the oceans where conventional soundings are not available. The method outlined here shows how the same VTPR radiances can be applied to mesoscale weather situations such as those over the Great Plains of the United States. Potentially, a sounding can be available at every VTPR scan spot at ~70 km resolution, if clouds do not prohibit obtaining a sounding to the earth's surface. This is a great increase in resolution from normal operational radiosonde soundings which are spaced approximately every 400 km in the western United States. In the operational retrieval of soundings over the oceans many adjacent scan spots of the VTPR are used in order to compensate for cloud-contaminated fields of view and to provide the best sounding without need for a "best" first guess profile. However, a single-field-of-view temperature retrieval algorithm, based on a best initial guess profile, is used here to obtain soundings at much higher resolution.

An important aspect is that a concurrent radiosonde sounding is used for the first guess. This is possible, in general, only over land, not over the oceans. Fritz (1977) has independently approached this method, which he terms the "adjustment method." For an excellent synopsis of the impact of satellite temperature soundings over oceans on large-scale weather forecasts, the reader is referred to Phillips (1976). A similar study of the impact of satellite data on mesoscale forecasts over land is in order and follows from the present study. At present, satellite soundings are available at 6–12 h intervals from the sun-synchronous NOAA and DMSP (Air Force) satellites. However, in 1980, temperature and moisture soundings of much higher frequency (i.e., 30 min to 3 h) will be available over the United States from the geostationary satellites (Suomi *et al.*, 1971).

Recent work has shown that mesoscale temperatures can be derived even in partly cloudy conditions (Hillger and Vonder Haar, 1976a,b). A cloud-correction technique based on a single field of view is able to provide suitable above-cloud soundings in some completely and partly cloudy situations. The technique proves to be too simple in complex cloud situations, and temperatures derived in cloud areas may remain cloud-contaminated. Cloud problem areas are pointed out and should be used with caution. Even if clouds

do significantly interfere with remote soundings, the use of high-resolution radiances does increase the possibility of sensing between clouds to obtain clear atmospheric temperatures. However, besides obtaining temperatures, mesoscale precipitable water (PW) fields are also realizable by eliminating temperature effects on the VTPR H_2O sounding channel. An application of these techniques is shown to provide mesoscale temperature and total precipitable water fields for 24 April 1975, a case study day for NASA's Atmospheric Variability Experiment (AVE) No. IV. (Hill and Turner, 1977).

2. Retrieval algorithm for NOAA VTPR applied to the mesoscale

The retrieval algorithm is based on a modified iterative type solution developed by Duncan (1974). To obtain the temperature profile of the atmosphere, one must find a solution $T(x)$ which satisfies the radiative transfer equation

$$N(\nu_i)=B[\nu_i,T(x_0)]\tau(\nu_i,x_0)+\int_{x_0}^{0} B[\nu_i,T(x)]\frac{\partial\tau(\nu_i,x)}{\partial x}dx \quad (1)$$

for each of the observed outgoing radiances $N(\nu_i)$ sensed by the satellite. The observed radiances are a product of the blackbody radiances B and the atmospheric transmittances $\tau(\nu_i,x)$ integrated from the surface, or cloud top, x_0 to the satellite along some vertical coordinate x. The blackbody radiances B are related directly to the temperature profile $T(x)$ and channel wavenumber ν_i by the Planck equation

$$B[\nu_i,T(x)]=\frac{C_1\nu_i^3}{\exp[C_2\nu_i/T(x)]-1}, \quad (2)$$

where C_1 and C_2 are known constants. Chahine (1968, 1970) applied the relaxation equation

$$B^{(n+1)}[\nu_i,T(x)]=\frac{\hat{N}(\nu_i)}{N^{(n)}(\nu_i)}B^{(n)}[\nu_i,T(x)] \quad (3)$$

to the radiative transfer equation to obtain an iterative solution for temperatures $T(x)$ at certain levels x, where the number of levels was equal to the number $\hat{N}$ of observed radiances. The observed radiances are thus used to fit the blackbody radiances B for each channel ν_i in successive iterations n, until the residuals between observed and calculated radiances

$$D_i^{(n)}=\hat{N}(\nu_i)-N^{(n)}(\nu_i) \quad (4)$$

for each channel reach an acceptable limiting value, usually the instrumental noise level.

This radiative transfer equation assumes a nonscattering atmosphere in local thermodynamic equilibrium. The dependence of the transmittances on changes in temperature is small compared to that of the Planck function so that the transmittances are calculated once before the first iteration to account for larger differences in initial guess temperature profiles.

Smith (1970) applied a relaxation formula based on radiance differences

$$B^{(n+1)}[\nu_i,T(x)]=[\hat{N}(\nu_i)-N^{(n)}(\nu_i)]+B^{(n)}[\nu_i,T(x)] \quad (5)$$

rather than radiance ratios. However instead of obtaining a solution at only specified levels x, independent estimates of the temperature profile $T(x)$ can be obtained for each channel ν_i through the Planck blackbody equation. The weights

$$W(\nu_i,x)=\partial\tau(\nu_i,x) \quad \text{for} \quad x\neq x_0$$
$$W(\nu_i,x_0)=\tau(\nu_i,x_0) \quad \text{for} \quad x=x_0$$

or derivatives of the transmittance are then used to compute a weighted average temperature $T(x)$ at each level x, i.e.,

$$T^{(n+1)}(x)=\frac{\sum_{i=1}^{6} T^{(n+1)}(\nu_i,x)W(\nu_i,x)}{\sum_{i=1}^{6} W(\nu_i,x)}. \quad (6)$$

In this case the six VTPR CO_2 channels are used to derive the entire temperature profile $T(x)$.

Smith *et al.* (1972) also used as his vertical coordinate $x=p^{2/7}$ divided into 100 equal levels in x from 0.01 mb to 1000 mb. This allows a temperature profile to be obtained which is not restricted to six atmospheric levels where the weighting functions are maximum. This method does not increase the information content of the radiances, but effectively allows a temperature determination at any desired level.

Duncan applied Chahine's relaxation formula (3) to Smith's independent temperature determinations in his retrieval algorithm. This is basically the same algorithm used in this study with modifications for input of any temperature profile as an initial guess sounding with an appropriate stratospheric profile above where the radiosonde sounding ends.

The VTPR instrument contains a water vapor and a window channel besides the six CO_2 channels as shown in Table 1 [for information on calculations of the transmittances see Weinreb and Neuendorffer (1973) and McMillin and Fleming (1970) for the H_2O and CO_2 transmittances, respectively]. The CO_2 transmittances are temperature-corrected by the initial guess profile using a second-degree polynomial representation according to the difference between the initial guess profile and a chosen standard atmosphere

TABLE 1. NOAA VTPR channels.

Channel number	Wavelength (μm)	Wavenumber (cm^{-1})	Approximate peak level of weighting function (mb)
CO_2 channels: 15 μm CO_2 absorption band			
1 (Q branch)	14.96	668.5	30
2	14.77	677.5	50
3	14.38	695.0	120
4	14.12	708.0	400
5	13.79	725.0	600
6	13.38	747.0	surface
H_2O channel: rotational water vapor absorption band			
7	18.69	535.0	600
Window channel: atmospheric window region			
8	11.97	833.0	surface

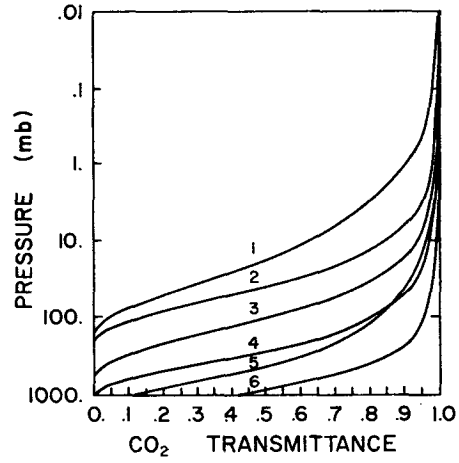

FIG. 1. VTPR CO_2 transmittances for U.S. Standard Atmosphere (Channels 1–6).

profile. Typical transmittances and weighting functions for the six CO_2 channels are shown in Figs. 1 and 2 for a U.S. standard atmosphere. The H_2O transmittances, however, are much more dependent on the initial guess profile than the CO_2 transmittances and are not shown here. Wark *et al.* (1974) have done some work with atmospheric water vapor which utilized the water vapor, window and lowest CO_2 channel. Other information on the VTPR instrument and the data archive format from which the data was obtained are explained in McMillin *et al.* (1973).

The retrieval of temperatures is a fairly straightforward process using the iterative method with up to 25 iterations for each profile to obtain a convergence noise level of less than 0.25 mW $(m^2\ sr\ cm^{-1})^{-1}$ for each of the six VTPR CO_2 channels. This convergence value is considered to be a limitation due to instrumental noise, and the reason for the cutoff at 25 iterations is due to a decreasing improvement in the radiance residuals with successive iterations at the expense of computer time.

3. Initial guess profile

The retrieval program was modified to provide mesoscale temperatures from calibrated radiances from NOAA VTPR archive data tapes and a suitable initial guess profile which has close proximity in space and time to the desired soundings. By using radiosonde soundings to create an initial guess we hoped to obtain reasonable retrieved profiles, because an iterative program, such as the one used, provides best resultant temperatures with a "best initial guess profile." A best initial guess profile should also aid to the cloud correction used, which depends on a good initial guess profile, as will be explained later.

The idea of a best initial guess profile is one that will allow the retrieval of temperature profiles which are most near the actual atmospheric temperature structure at the time of observation by the satellite. Even on this AVE experiment day there is a discrepancy between the radiosonde launch times which are used to compute initial guess profiles and the satellite overpass time of at least 1 or 2 h. During this time, since it is early morning, there usually is a large change in surface conditions as the morning surface inversion is broken or lifted. Also, the moisture changes rapidly during this time as vertical mixing takes place. Horizontal distances across the desired field may also reveal different types of air masses with differing lapse rates and moisture contents.

Because of physical limitations, temperature retrieval methods lack the vertical resolution to change small vertical features below the resolution of the weighting functions. In spite of this an attempt is not made to find the best initial guess for each air mass, but to

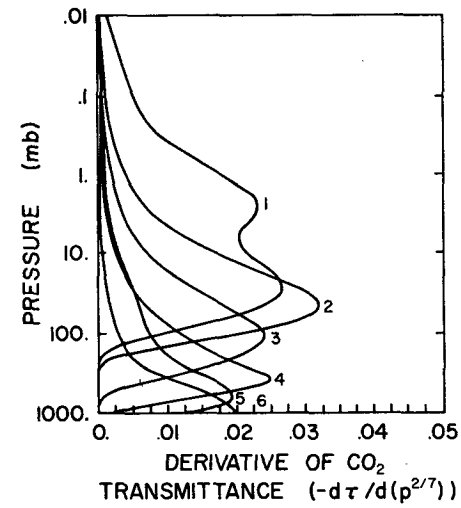

FIG. 2. As in Fig. 1 except for VTPR CO_2 weighting functions.

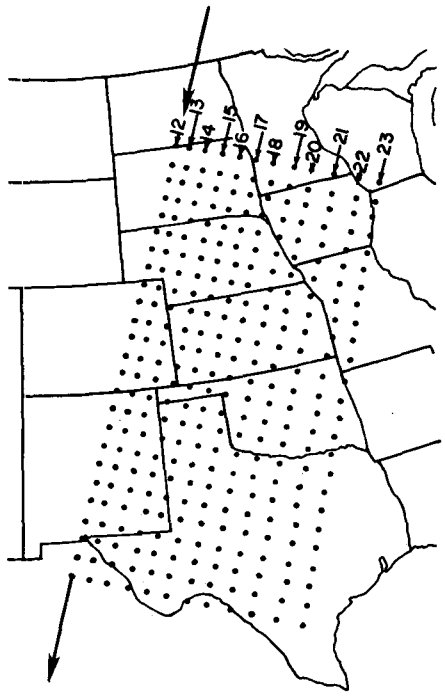

FIG. 3. VTPR scan coverage and resolution. Left half of several scan lines are shown (spots 12–23) for satellite pass over the Great Plains on 24 April 1975 at 1615 GMT.

provide one initial guess profile which should be applicable across the whole horizontal field desired. This may not be the best approach in many weather situations where air masses are widely different. However, by averaging a number of radiosonde soundings, features such as temperature inversions particular to individual radiosonde profiles should be smoothed out in the initial guess and features present across the whole field should be retained. Then, the same initial guess could be used to obtain the real or observed profile features through the iterations on the observed radiances without adding features particular to one radiosonde used as initial guess. Actually, Chahine (1968) proposed using an isothermal initial guess profile. However, in that case the transmittances would not be correctly initialized by the initial guess profile in terms of temperature lapse rates and total moisture content. A mean initial guess profile should then provide a best initial guess for the wide range of conditions on a certain day. Work is continuing on using two or more widely different initial guess profiles to try to optimize the desired effects of each profile.

The initial guess profiles used for 24 April 1975 were derived from special AVE radiosonde launches which provided soundings approximately every 3 h during the day. VTPR radiances were available at approximately 1615 GMT over the Great Plains from the morning or descending orbit of the NOAA 4 satellite. We used a space-averaged sounding derived from the radiosonde profiles as an initial guess profile for the area of the satellite pass shown in Fig. 3.

To obtain the space-averaged sounding required taking a set of radiosondes and weighting each one equally in an averaging program. All AVE radiosondes were given in 25 mb increments, so they were easily averaged. The main impact of this averaging was to smooth out small temperature inversions particular to specific areas and to make a mean mixing ratio profile which should be more moist than the driest sounding and drier than the most moist soundings. This average sounding is a rather smooth vertical profile and will not reproduce small temperature inversions when used as an initial guess in the retrieval algorithm. Also, since the mean moisture profile will be too dry in the moist air mass it will cause temperatures to be retrieved that are too cool in very low levels. Moisture makes the observed radiances low, therefore causing low retrieved temperatures near the H_2O weighting functions peak, usually at or below 700 mb. On the other hand, the mean profile will be too moist in the dry region causing higher temperatures than with a correct moisture profile. These temperature differences are being studied as another approach toward moisture determination using the CO_2 channels alone.

The initial guess profile that was used was obtained by averaging ten 1800 GMT radiosonde profiles from the AVE radiosonde network shown in Fig. 4. Likewise a 1500 GMT mean profile was also computed from all 10 radiosondes, but the 1800 GMT profile was chosen as an initial guess because of higher surface

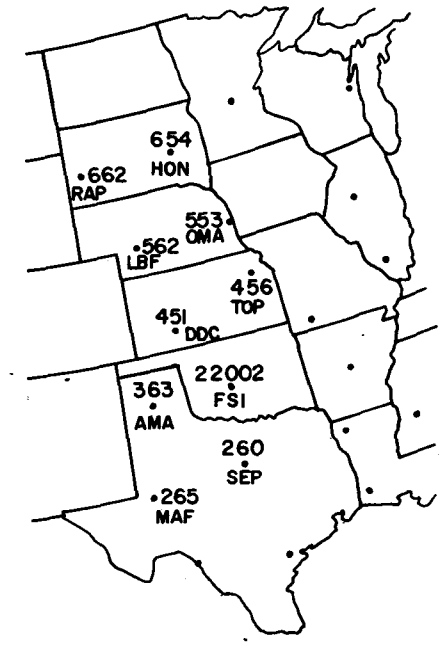

FIG. 4. Location of radiosonde launch sites for AVE IV experiment on 24 April 1975.

temperatures and lack of a surface temperature inversion. The difference between the two mean profiles was less than 1.0°C except below 850 mb where the temperature was 2.5°C larger at the surface in the 1800 mean profile than the 1500 mean. The main reason for choosing this profile was to aid the cloud correction technique explained below.

Another mean profile was also calculated at 1500 GMT. Besides the one containing all ten stations, a mean using only the six southern stations in Fig. 4 was also used as an initial guess in a small sample of 27 soundings scattered from north to south. The results of comparisons between temperature and moisture values using each mean profile as an initial guess are shown in Table 2. For case A with 10 and 6 profiles, respectively, in the mean, the main difference in the initial guess profiles was generally warmer temperatures by 2–3°C in the southern mean profile below 200 mb (tropopause) and cooler temperatures above the tropopause. This is caused by a higher tropopause in the southern mean. In spite of this difference, the derived profiles give 500 mb temperatures which are only 1.4°C warmer using the southern initial guess, whereas the initial guess difference was 2.6°C at 500 mb. The retrieved temperature profiles are affected by the initial guess, but a correlation of 0.95 between two samples of 500 mb temperatures for 27 profiles shows a high degree of reproducibility of the field structure in spite of two different initial guesses, even in cloudy cases included in the sample.

The difference in initial guess total precipitable water for the two profiles was negligible and a correlation of 0.99 between the two data samples results in spite of the difference in temperature profiles for the two initial guesses.

Case B is a similar comparison between the two previously mentioned mean profiles created using all 10 profiles at 1500 and 1800 GMT, respectively. The difference in the initial guess profiles was smaller here and the correlation was higher for the two samples of 500 mb temperatures. These comparisons show that the obtained horizontal field structure is not highly dependent on the initial guesses tested here. Other initial guesses with different lapse rates and different moisture profiles should exhibit larger differences in the derived profiles.

TABLE 2. Results of using different mean profiles as initial guess.

	Case A*	Case B**
RMS difference between mean profiles for 38 levels (25 to 950 mb)	2.8°C	0.8°C
RMS difference between 500 mb temperatures derived using each initial guess profile for 27 sample profiles	1.4°C	0.7°C
Initial guess difference at 500 mb	(2.6°C)	(0.8°C)
Correlation coefficient for 500 mb temperatures from two samples	0.95	0.99
Total precipitable water (PW) (1) in each initial guess (2)	1.88 cm 1.96 cm	1.88 cm 1.87 cm
Correlation coefficient for PW values from two samples	0.99	0.99

* Case A. Comparison using mean profiles at 1500 GMT, one containing all ten radiosondes (1) and the other only the six southern radiosondes (2) in the mean.

** Case B. Comparison using mean profiles at 1500 GMT (1) and 1800 GMT (2), each containing all ten radiosondes in the mean.

4. Cloud correction technique

The cloud correction is a modification of a technique used by Shaw *et al.* (1970). The technique is not intended to be sophisticated, but to correct for cloudy situations which are most easily identifiable, single cloud layers. The cloud layer is assumed to be completely overcast, and if not overcast, a lower than actual cloud level will result. Although this cloud correction technique does not work well in many situations with small cloud amounts or high or multi-level clouds, it does eliminate problems with some cloudy fields of view, thereby producing more horizontally homogeneous temperatures compared to nearby non-cloudy columns at and slightly above the calculated cloud level than with no correction.

Basically the idea relies on a best initial guess profile and integrated radiances derived from it through the radiative transfer equation (1). These integrated radiances are then compared to observed radiances for three VTPR CO_2 channels whose weighting functions peak lowest in the atmosphere (channels 4, 5 and 6). If the rms residual between the observed and calculated radiances is large, then the observed radiances are probably cloud-contaminated and have low values. The hypothesized cloud level is then raised in increments and the radiances are again calculated and compared until the rms radiance residual reaches a minimum, meaning that the calculated radiances are now smaller than the observed radiances, or that an effective cloud-top level has been attained. Using the 1800 mean profile as an initial guess instead of the 1500 mean aided the cloud correction technique. The higher lapse rate near the surface at 1800 GMT made the determination of the effective cloud level easier. If a temperature inversion were present the rms radiance residual would reach a temporary minimum value at that level, falsely underestimating the cloud-caused minimum, which may be at a higher level.

The use of a best initial guess profile will also aid this method by producing calculated radiances nearly like those of the desired profile in a clear atmosphere.

A similar technique was used by Hodges (1976) in a cloud model in an attempt to also obtain cloud amount information. The technique used here will be valid only for overcast situations unless a fractional cloud cover is assumed. In this case, since 100% cloud cover is assumed, the cloud level will be at a minimum or lower height in order to make the rms radiance residual a minimum. Temperature soundings are then obtained above this effective cloud level through the iterative process previously outlined.

5. Integrated moisture values

To obtain precipitable water values a slightly more involved method was required. The idea was to compare observed H_2O channel (channel 7) radiances with radiances calculated using the radiative transfer equation on the derived temperature profiles with a known initial guess precipitable water amount. The comparison was done after the iterative process was used to obtain the temperature profiles in order to try to compensate for horizontal temperature changes in each scan spot across the derived field.

The H_2O channel radiance is strongly dependent on both total atmospheric moisture and temperature, but by reducing or eliminating the temperature effect on the H_2O radiance, the result should be correlated with conventional precipitable water values obtained at the standard radiosonde sites. The H_2O radiance residual, as it is called here, is a difference between the observed H_2O channel radiance and the calculated H_2O channel radiance using the iterated or derived temperature profile

$$H_2O\ \text{Residual} = N_{\text{obs}}(T_a, PW_a) - N_{\text{calc}}(T_i, PW_0) \quad [H_2O\ \text{channel}]$$

where:

T_a actual temperature profile
PW_a actual precipitable water amount
T_i iterated temperature profile
PW_0 initial guess precipitable water amount ($\sim$2 cm for 24 April 1975 18 GMT mean initial guess sounding).

The initial guess precipitable water amount is a constant value which is not changed in the iterative process. Now, if the iterated temperature profile approximates the actual profile, i.e., $T_i \approx T_a$, then the difference between the calculated and observed radiances will be a function only of the difference between actual and initial guess precipitable water amounts:

$$H_2O\ \text{Residual} \propto PW_a - PW_0 \propto PW_a.$$

This radiance residual is, however, just proportional to the actual precipitable water amount PW_a since the initial guess moisture content PW_0 was constant throughout the iteration process for all derived profiles. The H_2O channel radiance is used solely for the determination of precipitable water amounts. A least-squares linear regression between this H_2O radiance residual and the precipitable water values at the radiosonde sites gives a high correlation, as will be shown.

Looking back at Table 2, we see in case A that the derived 500 mb temperatures using each initial guess profile had an rms difference of 1.4°C. Values for other lower levels tended to be larger where the initial guess profiles were most different. However, the derived precipitable water values were still highly correlated at 0.99. At least for the mean initial guess profiles used here, there appears to be little effect of the initial guess on the structure of the obtained total precipitable water values. Larger rms differences in initial guess profiles should again display correspondingly larger rms differences in the resultant derived temperature profiles, but only initial guess profiles with different vertical temperature structure should display a lower correlation in derived total moisture values. Again, work is expanding into the testing of different initial guess profiles to optimize the resultant horizontal structure of the moisture fields. A better feeling for errors in the moisture content can be seen by looking at the linear least-squares line fit shown with the precipitable water results.

6. 24 April 1975 results

The AVE experiment day, 24 April 1975, proved to be quite interesting and also provide radiosonde soundings at time periods near the satellite overpass at 1615 GMT. The surface weather observations for 1600 are plotted using the standard station model in Fig. 5 for the most interesting area centered in Oklahoma. The surface dry tongue extending through the panhandle of Texas into Oklahoma presents a strong moisture gradient along the dry line to its south. The most important features in this figure are the observed cloud cover shown in the stippled regions and the isopleths of surface dew point temperature. These isodrosotherms will later be shown to be reproduced quite well by the integrated moisture values obtained from the VTPR H_2O channel.

Fig. 6 shows the Synchronous Meteorological Satellite (SMS) visible image for this case study day at 1600 GMT. Northern Texas and most of Oklahoma are clear. Cloud cover is extensive in Kansas, and partly cloudy conditions in southern Texas will be shown below to affect the derived temperatures there.

7. Derived 500 mb temperatures on the mesoscale

Temperatures obtained through iterations on the mean initial guess profile were plotted according to their calculated horizontal positions for certain pressure

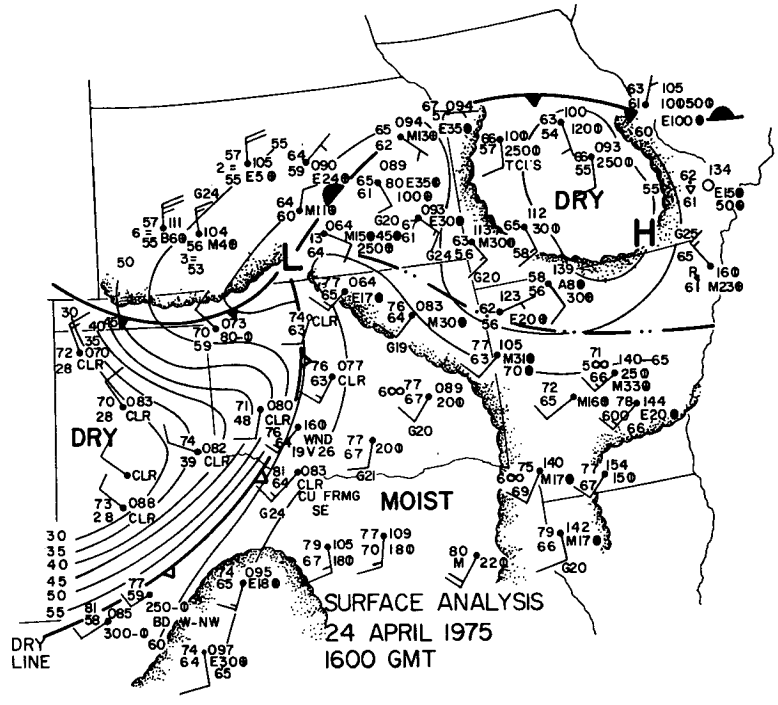

FIG. 5. Surface observations plotted according to standard station model. Isopleths of dew point temperature are analyzed and stippled regions indicate clouds.

levels and analyzed. An earth location algorithm involving spherical geometry was used to calculate individual scan spot positions from satellite orbit parameters. The 500 mb temperatures are characteristic of the mesoscale temperature fields which satellite sounders are capable of producing. Higher tropospheric levels contain less temperature variation, and lower levels are plagued both by clouds and the unchanging initial guess moisture profile used. Since temperature profiles were derived only above the calculated cloud level, the 700 mb temperatures, for example, were unobtainable in many cloudy columns. The 700 mb temperatures were also too high in the dry tongue area due to the effect of the dry atmosphere on the VTPR CO_2 channels with lowest weighting function peaks. The dryness, as explained earlier, causes observed radiances to be high and therefore causes temperatures derived from these observed radiances to be high when the moisture content is kept constant in the iteration process.

Fig. 7 shows the derived 500 mb temperatures at 1615 GMT. The contours were analyzed from about 200 temperature soundings obtained at almost every scan spot of the VTPR instrument over this region. The initial guess 500 mb temperature was about −15°C, corresponding to a mean temperature on the Kansas-Oklahoma border at this level. The individually derived temperature values at 500 mb are shown to indicate data coverage and resolution and to give a feel for the random noise in the temperatures.

The 500 mb temperature analyses obtained from the radiosonde soundings alone are shown in Figs. 8 and 9. The first figure contains the 500 mb temperatures from AVE radiosonde launches at a time period before the satellite pass at 1500 GMT and the second contains the radiosonde launches for the period 3 h later (1800 GMT) after the satellite pass. Both figures are fairly consistent with only a slight warming in the 1800 GMT 500 mb temperatures and a slight shift of the cold trough axis to the east.

When compared to the radiosonde analyses, the

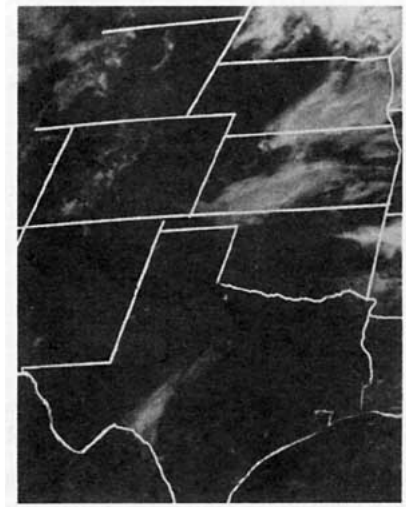

FIG. 6. SMS visible image for 24 April 1975 at 1600 GMT.

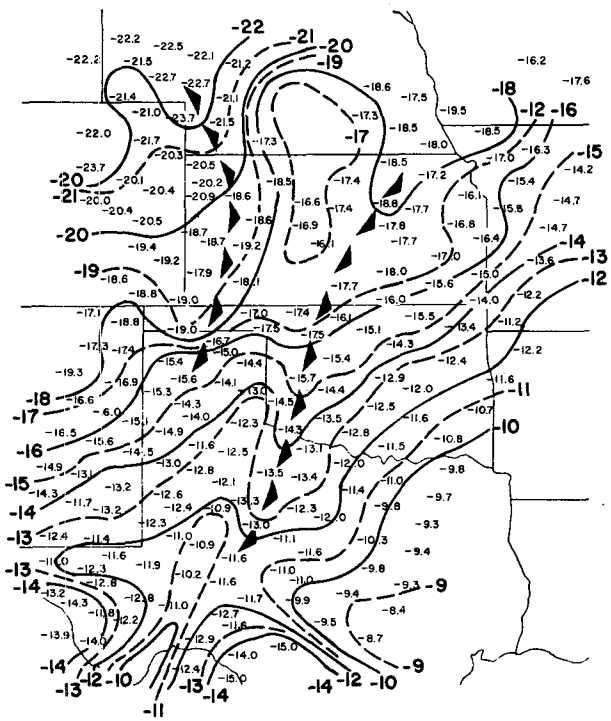

FIG. 7. Satellite-derived 500 mb temperature field obtained using an iterative retrieval algorithm with a mean radiosonde sounding as initial guess profile. Numbers at scan spot positions indicate data coverage and resolution.

satellite-derived temperatures in Fig. 7 appear in general to be biased too low by about 1–2°C. This is probably due to the vertical structure or magnitude of the mean initial guess temperature profile used, or to the transmittances which are corrected for temperature and moisture by the initial guess profile. The initial guess temperature profile has a strong compounding influence since it is used both as an initial guess and to calibrate the transmittances. (Associating the bias to the initial guess profiles also assumes that the observed radiances are calibrated correctly.) Using the mean profile created from the six southern stations at 1500 or 1800 GMT instead of for all ten stations should have raised the derived temperatures at 500 mb and reduced the bias in the analyzed field. However, the absolute values are not as important as the relative temperature changes, especially the horizontal temperature structure at the mesoscale. Absolute temperature values are not needed to determine significant horizontal changes across the temperature field. The cold trough axis does appear in central Oklahoma about where it is also shown in the radiosonde analyses. Any difference in the actual axis location between the two data sets is probably due to the difference in horizontal resolution capabilities of the two data sets. Since the satellite-derived temperatures are more densely spaced by a factor of about 36, the trough axis is probably more correctly placed by this much denser satellite data network.

Two main problem areas caused by clouds exist in this particular 500 mb analysis. The low temperature regions of −14°C in southern Texas are caused by cloud contamination which was not sufficiently dealt with by the simple cloud corrections technique. These scan spots contain small cloud amounts which are handled least effectively by the cloud correction technique when complete cloud cover is assumed. The effective cloud level was placed at too low a level, causing derived temperature to be low by 3–4°C above the assumed cloud level. However, by knowing that these cases are biased too low by clouds they can hopefully be eliminated. Also in Kansas where clouds do become thicker, the ability to obtain soundings does decrease. The horizontal resolution capability is reduced by clouds extending up to and above 500 mb. Here again, where the 500 mb temperatures are obtained in cases with small cloud amounts, they are biased too low because of the assumed 100% cloud amount in only slightly cloudy columns. The position of the effective cloud level is critical to the cloud correction technique used here, and the effect of clouds

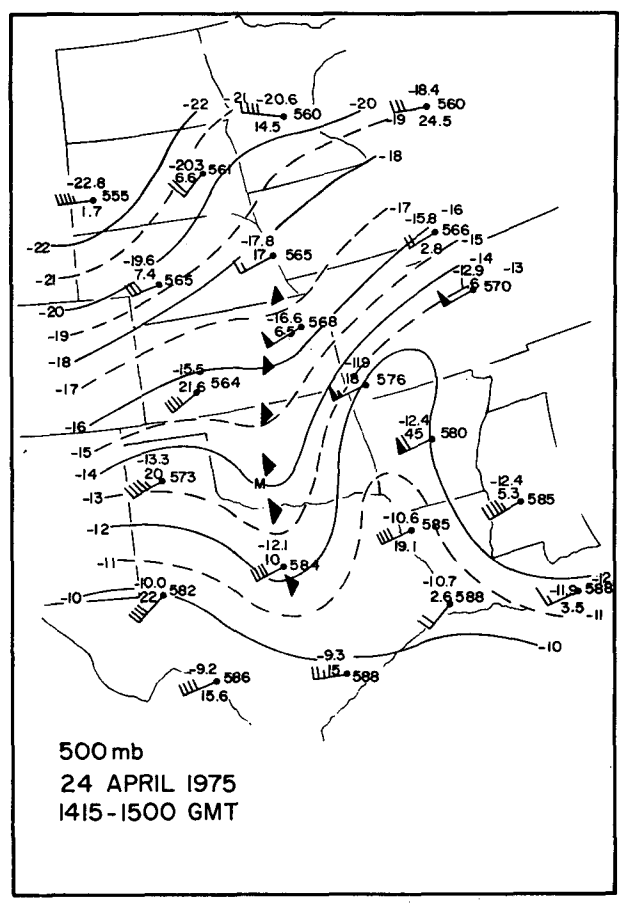

FIG. 8. Radiosonde 500 mb temperatures at ~1500 GMT.

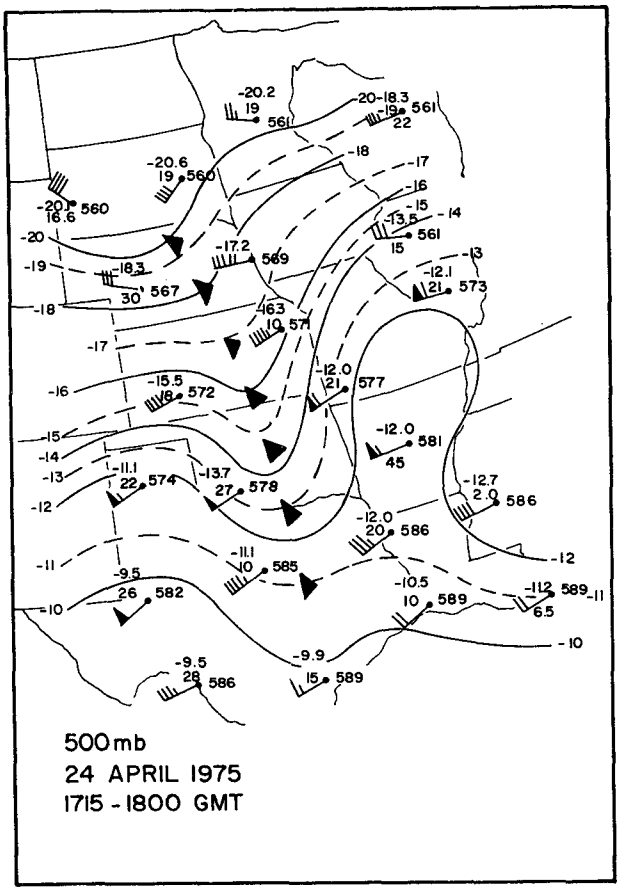

FIG. 9. Radiosonde 500 mb temperatures at ~1800 GMT.

can be summed up as mainly increasing the variability of temperatures derived under cloudy situations.

An example of the effect of small cloud amounts is the region in southeastern Colorado and western Kansas where the isotherms are bent towards lower temperatures. This feature does not show up in the radiosonde analyses alone and is associated with the small cloud amounts there. Other temperature features which occur in clear areas are associated with the observed radiances and not the cloud correction technique. Also, multi-level and high-cloud situations, such as in central Nebraska and Kansas, lead to temperatures which are too warm. The simple cloud correction should not be expected to work in such complex cloud situations.

These two problem areas show the need for an assumed cloud amount parameter in this simple cloud-corrections technique, especially small cloud amount cases. In cases with small cloud amounts, the effective cloud level is much lower than the actual partial cloud level. This causes temperatures above this effective cloud level to be biased too low due to an isothermal temperature tendency of the derived profiles below the cloud level when no cloud is assumed (Chahine, 1970). The derived temperatures below the actual cloud level tend toward the cloud top temperature when the observed radiances originate from a completely overcast column.

The idea behind using this cloud correction technique was to try to obtain more horizontal temperature resolution in cases where the vertical column was not completely clear. Over half of the derived temperatures were obtained from completely clear columns, but a certain amount of horizontal resolution would have been lost by throwing out all cloudy columns. Rather, the cloud correction was applied and its effects on derived temperatures are pointed out to show that it is least effective in cases with small but detectable cloud amounts and in high or multi-level cloud situations. So, unless the cloud situation is known, this simple cloud correction technique provides little extra value to the clear soundings alone. For this reason, an independent visible or infrared channel, from which cloud amount information can be extracted, should be available along with the satellite sounding radiances. Such information will be available from the new generation of sounding instruments to be launched on the operational NOAA satellites in the 1980's.

8. Precipitable water field on the mesoscale

Perhaps the most interesting and useful analysis obtained is the precipitable water (PW) analysis in

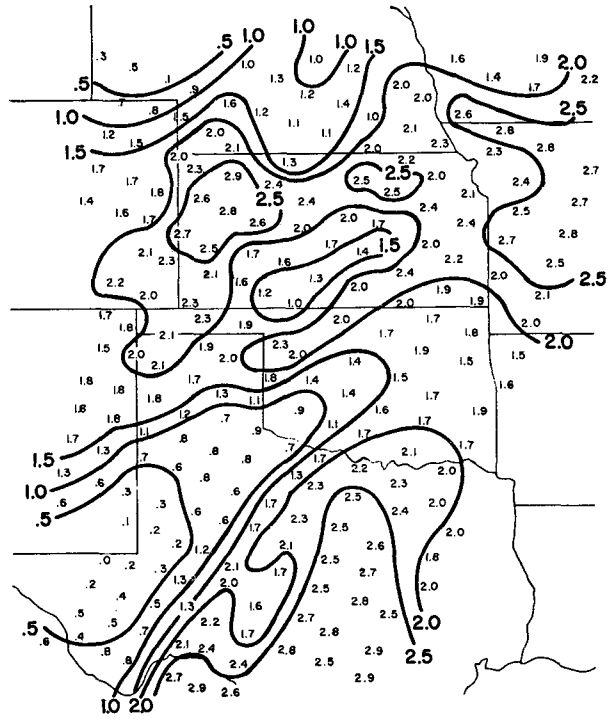

FIG. 10. Satellite-derived precipitable water field obtained using a least-squares linear regression of radiosonde total precipitable water values against H_2O radiance residuals. Numbers indicate data coverage and resolution.

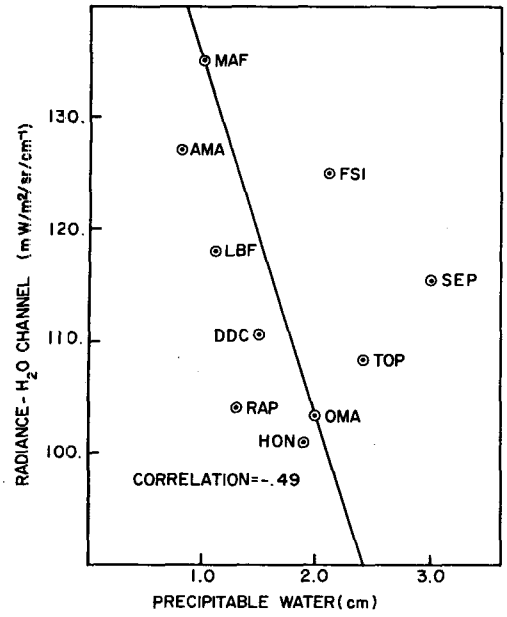

FIG. 11. H_2O channel radiances plotted against time-interpolated precipitable water values at radiosonde sites in the study area.

Fig. 10. The procedure explained earlier was used to try to eliminate the temperature effect on the VTPR H_2O channel by using the derived temperature profiles to obtain calculated radiances. If the derived temperatures are reasonably accurate then differences between observed and calculated radiances would be due to moisture effects only. This is shown graphically in Figs. 11 and 12, where H_2O channel radiances and H_2O channel radiance residuals are plotted against time-interpolated PW values at the AVE radiosonde sites. In order to obtain a larger set of data points for comparison, the field of derived satellite soundings was extended up into the northern Great Plains. PW values at approximately 1500 and 1800 GMT were used to obtain time-interpolated PW values at 1615 GMT which were then plotted against the radiance values from the H_2O channel and the H_2O radiance residuals.

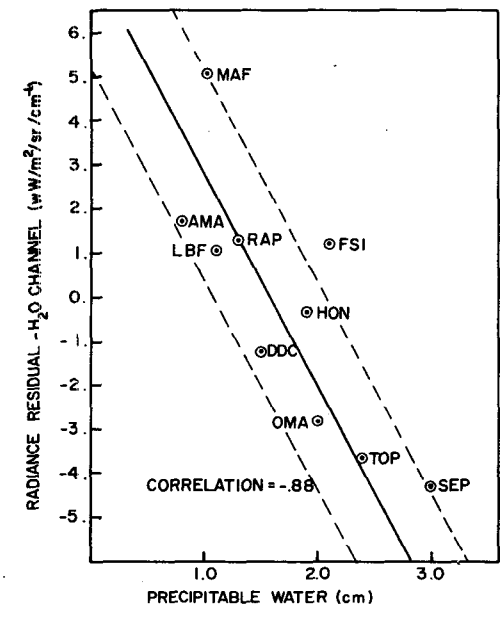

FIG. 12. As in Fig. 11 except for H_2O radiance residuals.

When plotted against the H_2O channel radiances, the PW values produced only a -0.49 correlation. Large radiances are correlated with low PW amounts, but are also strongly dependent on temperature. This is seen in the general arrangement of the radiosonde stations with highest temperatures also having the largest H_2O channel radiances. The southern, or warmer, stations in Fig. 11 are in the top of the graph and the least-squares line fit shows a steep slope which is only weakly dependent on the PW amount.

However, in Fig. 12, by trying to eliminate the temperature effect on the H_2O channel radiance, the stations are not arranged preferentially according to temperature, but arranged in terms of PW amounts. The slope of the least squares line fit shows much more variation explained by PW changes than in Fig. 11. The rather high correlation of -0.88 excludes the station FSI (Fort Sill, Okla.) which did not have a sounding launch at 1500 GMT. This point was not used because it could not be treated as the others to obtain an interpolated PW value at 1615 GMT.

Because of the high correlation, a least-squares linear regression was used to calculate coefficients to convert H_2O radiance residuals directly into the PW values plotted in Fig. 10. The scatter of time-interpolated PW values about the regression line, except for FSI, is less than 0.5 cm of H_2O which can be considered a maximum error level for this data set. Dashed lines at ± 0.5 cm from the line fit encompass all values except for FSI.

The only high-resolution data set to compare with these PW values are the surface observations in Fig. 5. The surface dry tongue through Texas into Oklahoma is shown in the satellite derived field by a large change in PW values from less than 0.5 cm in western Texas to over 2.5 cm of H_2O in eastern Texas. The surface dry line oriented southwest to northeast is designated by a strong PW gradient of about 1 cm of H_2O per 70 km, the linear distance between scan spot centers.

The moist areas in eastern Texas and western Kansas in the surface observations contain over 2.5 cm of PW. However, the dry region in central Kansas of less than 1.5 cm of PW is caused by cloud contamination up to and above the 500 mb level. In this case the radiances are integrated from vertical columns truncated by the high cloud levels. As expected, this causes the radiance residuals to be low because of the decreased difference between observed and calculated radiances which arises mainly from H_2O differences

in the low levels. Clouds do, therefore, cause some contamination of these data but the PW values seem to be mostly unaffected unless cloud levels are high. In southern Texas where lower clouds caused 500 mb temperatures to be low, the PW values seem to be unaffected compared to neighboring scan spots. High PW values here agree with small dew point depression values in the surface observations.

These two data sets (Figs. 5 and 10) should not be correlated exactly since one is for surface values and the other for integrated moisture. However, since moisture in the atmosphere is concentrated near the surface, there should be some indication of PW amounts in the surface dew point temperatures (Smith, 1966). Differences in the two moisture analyses should yield an indication of vertical mixing of moisture provided the data sets were obtained at the same time. High surface dew point temperatures and low PW values would indicate little vertical mixing, whereas higher PW values with the same surface moisture would indicate more vertical mixing.

Moisture features such as the indicated dry line feature or moisture gradient in the derived PW values are extremely important to forecasting convective storm development. The horizontal position of the dry line usually determines a line along which the most severe storms occur. The dry line feature and vertical moisture mixing information together could help pinpoint subsequent convective development later in the day.

9. Conclusions

High-resolution temperature and moisture information is necessary for mesoscale weather analysis and forecasting. The ability to provide such mesoscale information is shown to be feasible now, from existing operational satellite sounding radiances over the United States. Even though the derived temperature values are biased by cloud contamination in certain areas, they do show significant relative horizontal changes in non-cloudy areas, which for example can better locate cold trough positions.

Precipitable water information is probably the most needed information on the mesoscale. Moisture varies more rapidly in space and time than temperature at smaller scales. Precipitable water values derived from the NOAA VTPR H_2O channel, when corrected for temperature effects, provide a reliable source of horizontal moisture information. Cloud contamination which lowers temperature values does not significantly affect the derived integrated moisture amounts beyond the maximum noise level of 0.5 cm of H_2O except in high cloud cases.

An important aspect of the present study, in contrast to earlier large-scale temperature soundings from satellites over the oceans, is the use of concurrent satellite and radiosonde data in a joint analysis. The more widely spaced radiosondes, with their good vertical resolution, may be considered the trunks of the data set; the higher horizontal resolution satellite data (the branches) are coupled to and dependent upon the trunks. No attempt has yet been made of optimum analysis and assimilation of the data sets. That study, as well as preparation to add the fourth dimension (time) from upcoming high-frequency geostationary satellite sounders will be the subject of considerable future research. If information on temperature and moisture does become routinely available from satellite soundings for mesoscale analysis and forecasting, it will provide a valuable additional tool to conventional radiosonde sounding information alone.

Acknowledgments. Special thanks go to Robert Maddox of the APCL/NOAA labs in Boulder for analyzing the surface and 500 mb maps used for this case study day. Dr. L. Duncan at the U.S. Army White Sands Missile Range provided help in initiating the iterative temperature retrieval program, and additional technical assistance and data were obtained from the Indirect Soundings Branch of NOAA/NESS.

Funding for this research was received from NASA, Contract NGR-06-002-102, and the Bureau of Reclamation, Contract 6-07-DR-20020.

REFERENCES

Chahine, M. T., 1968: Determination of the temperature profile in an atmosphere from its outgoing radiance. *J. Opt. Soc. Amer.*, **58**, 1634–1637.

——, 1970: Inverse problems in radiative transfer: Determination of atmospheric parameters. *J. Atmos. Sci.*, **27**, 960–967.

Duncan, Louis D., 1974: An iterative inversion of the radiative transfer equation for temperature profiles. R & D Tech. Rep. ECOM-5534, Atmos. Sci. Lab., White Sands Missile Range, New Mexico, 18 pp. [NTIS Ref. AD-776 899/7GI].

Fritz, Sigmund, 1977: Temperature retrievals from satellite radiance measurements—an empirical method. *J. Appl. Meteor.*, **16**, 172–176.

Hill, Kelly, and Robert E. Turner, 1977: NASA's atmospheric variability experiments (AVE). *Bull. Amer. Meteor. Soc.*, **58**, 170–172.

Hillger, Donald W., and Thomas H. Vonder Haar, 1976a: Mesoscale temperature and moisture fields from satellite infrared soundings. Atmos. Sci. Pap. No. 249, Colorado State University [NTIS Ref. number applied for].

——, and ——, 1976b: Mesoscale temperature and moisture fields from satellite infrared soundings. *Proc. Meteorological Observations from Space: Their Contribution to the First GARP Global Experiment*, COSPAR, Philadelphia, June, 59–63 [NTIS Ref. PB 262 530/AS].

Hodges, Donald B., 1976: A single field of view method for retrieving tropospheric temperature profiles from cloud-contaminated radiance data. NASA Contractor Report, NASA CR-2726, 90 pp. [NTIS Ref. N76-29861/1GI].

McMillin, L. M., D. Q. Wark, J. M. Siomkajlo, P. G. Abel, A. Werbowetzki, L. A. Lauritson, J. A. Pritchard, D. S. Crosby, H. M. Woolf, R. C. Luebbe, M. P. Weinreb, H. E. Fleming, F. E. Bittner and C. M. Hayden, 1973: Satellite infrared soundings from NOAA spacecraft. NOAA Tech. Rep. NESS 65, 112 pp. [NTIS Ref. COM-73-50936/6AS].

——, and H. E. Fleming, 1976: Atmospheric transmittance of an absorbing gas: A computationally fast and accurate

transmittance model for the absorbing gases with constant mixing ratios in inhomogeneous atmosphere. *Appl. Opt.*, **15**, 358–363.

Phillips, Norman A., 1976: The impact of synoptic observing and analysis systems on flow pattern forecasts. *Bull. Amer. Meteor. Soc.*, **57**, 1225–1240.

Shaw, J. H., M. T. Chahine, C. B. Farmer, L. D. Kaplan, R. A. McClatchey and P. W. Schaper, 1970: Atmospheric and surface properties from spectral radiance observations in the 4.3 micron region. *J. Atmos. Sci.*, **27**, 773–780.

Smith, W. L., 1966: Note on the relationship between total precipitable water and surface dew point. *J. Appl. Meteor.*, **5**, 726–727.

——, 1970: Iterative solution of the radiative transfer equation for the temperature and absorbing gas profile of an atmosphere. *Appl. Opt.*, **9**, 1993–1999.

——, H. M. Woolf and H. E. Fleming, 1972: Retrieval of atmospheric temperature profiles from satellite measurements for dynamical forecasting. *J. Appl. Meteor.*, **11**, 113–122.

Suomi, V., T. Vonder Haar, R. Kraus and A. Stam, 1971: Possibilities for sounding the atmosphere from a geosynchronous spacecraft. *Space Research XI*, Academie-Verlag, 609–617.

Wark, D. Q., J. H. Lienesch and M. P. Weinreb, 1974: Satellite observations of atmospheric water vapor. *Appl. Opt.*, **13**, 507–511.

Weinreb, M. P., and A. C. Neuendorffer, 1973: Method to apply homogeneous-path transmittance models to inhomogeneous atmospheres. *J. Atmos. Sci.*, **30**, 662–666.